Mean first passage times and Eyring–Kramers formula for fluctuating hydrodynamics

OPEN ACCESS

Journal of Statistical Mechanics: Theory and Experiment
An IOP and SISSA journal

PAPER: Classical statistical mechanics, equilibrium and non-equilibrium

Mean first passage times and Eyring–Kramers formula for fluctuating hydrodynamics

Jingbang Liu[1,2], James E Sprittles[1] and Tobias Grafke[1,*]

[1] Mathematics Institute,University of Warwick, Coventry CV4 7AL, United Kingdom
[2] Department of Mathematics, University of Oslo, Oslo 0851, Norway
E-mail: T.Grafke@warwick.ac.uk, jingbanl@.uio.no and J.E.Sprittles@Warwick.ac.uk

Received 15 May 2024
Accepted for publication 18 September 2024
Published 30 October 2024

Online at stacks.iop.org/JSTAT/2024/103206
https://doi.org/10.1088/1742-5468/ad8075

Abstract. Thermally activated phenomena in physics and chemistry, such as conformational changes in biomolecules, liquid film rupture, or ferromagnetic field reversal, are often associated with exponentially long transition times described by Arrhenius' law. The associated subexponential prefactor, given by the Eyring–Kramers formula, has recently been rigorously derived for systems in detailed balance, resulting in a sharp limiting estimate for transition times and reaction rates. Unfortunately, this formula does not trivially apply to systems with conserved quantities, which are ubiquitous in the sciences: The associated zeromodes lead to divergences in the prefactor. We demonstrate how a generalised formula can be derived, and show its applicability to a wide range of systems, including stochastic partial differential equations from fluctuating hydrodynamics, with applications in rupture of nanofilm coatings and social segregation in socioeconomics.

Keywords: metastable states, large deviation, molecular dynamics

*Author to whom any correspondence should be addressed.

Contents

1. Introduction

Metastability is a well-known phenomenon appearing in many areas of natural sciences: A stochastic system spends a long time near some typical configuration, but can rarely switch (transition) to a drastically different configuration. The corresponding waiting times are known to be exponentially large in the noise strength.

The typical picture is that of a stochastic diffusion in a potential landscape, where local minima correspond to long-lived states. Fluctuations can then push the system across a potential barrier into another local minimum, in which it will remain for long times. While chemical reactions, conformational changes in biomolecules, protein folding, or magnetic field reversal in ferromagnets are well-known examples of this phenomenon, similar ideas can be found in rather broad areas of science, such as in brain activity [1], quenched disorder in semiconductors [2], tipping points in Earth's climate [3] including warm-water currents in the north Atlantic [4], or ecosystem collapse [5].

J. Stat. Mech. (2024) 103206

Concretely, take the gradient diffusion for $X_t \in \mathbb{R}^n$,

$$\mathrm{d}X_t = -\nabla U\left(X_t\right)\mathrm{d}t + \sqrt{2\varepsilon}\,\mathrm{d}W_t\,, \tag{1}$$

where $U : \mathbb{R}^n \to \mathbb{R}$ is the potential, and W_t white-in-time Brownian motion. For this system and in the limit of small noise, $\varepsilon \to 0$, transitions between two local minima x_- and x_+ of $U(x)$, under some assumptions on the potential [6], must happen through a saddle point x_s, and the expected transition time τ is given by the *Eyring–Kramers* formula

$$\tau = \frac{2\pi}{|\lambda_-|}\sqrt{\frac{|\det H_s|}{\det H_-}}\mathrm{e}^{\Delta U/\varepsilon} \tag{2}$$

asymptotically sharp in the limit of vanishing ε. Here, $H_- = \nabla\nabla U(x_-)$ and $H_s = \nabla\nabla U(x_s)$ are the Hessian of the potential U at the starting fixed point x_- and at the saddle x_s , respectively, and λ_- is the single negative eigenvalue of H_s, corresponding to the single unstable direction of the saddle point. The exponential scaling with the energy barrier height $\Delta U = U(x_s) - U(x_-)$ is known as *Arrhenius' law* [7], and can be made rigorous within sample path large deviation theory as established in [8] in more general cases than just gradient diffusions. The pre-exponential factor is also known for almost a century [9, 10], but has only recently been proven rigorously [6, 11–14]. Within these works, it is possible to consider the more general case of a diffusion in a potential landscape with *mobility* $M(x) : \mathbb{R}^n \to \mathbb{R}^{n\times n}$, which is positive definite and symmetric, via

$$\mathrm{d}X_t = -M\left(X_t\right)\nabla U\left(X_t\right)\mathrm{d}t + \varepsilon\nabla\cdot M\left(X_t\right)\mathrm{d}t + \sqrt{2\varepsilon}M_{1/2}\left(X_t\right)\mathrm{d}W_t\,, \tag{3}$$

where $M_{1/2}(x) : \mathbb{R}^n \to \mathbb{R}^{n\times n}$ is the unique positive definite matrix for which $M_{1/2}M_{1/2}^T = M$ and $(\nabla\cdot M)_j(x) = \sum_i \partial_{x_i} M_{ij}(x)$. In this case, the Eyring–Kramers formula reads [14]

$$\tau = \frac{2\pi}{\mu_-}\sqrt{\frac{|\det H_s|}{\det H_-}}\mathrm{e}^{\Delta U/\varepsilon}\,, \tag{4}$$

where μ_- is the unique negative eigenvalue of the matrix $M(x_s)H_s$.

While the generalised gradient diffusion with mobility (3) can still be interpreted as system that minimises the potential U, just with a position dependent metric given by the mobility, it opens up a much wider class of physical phenomena beyond the overdamped Langevin equation (1). In particular, if further generalizing to the functional setup and allowing generalised gradient diffusions in function spaces or spaces of probability measures, it includes hydrodynamic limits of interacting particle systems, lattice gases, pedestrian dynamics, traffic flow, etc, all of which can be seen as (functional) gradient flows of some entropy functional for a (generalised) Wasserstein metric [15]. For example, the large number of particles limit of many non-interacting random walkers is given by the stochastic diffusion equation for a density $\rho(x,t)$,

$$\partial_t\rho = \Delta\rho + \sqrt{2\varepsilon}\nabla\cdot\left(\sqrt{\rho}\eta\right)\,,$$

J. Stat. Mech. (2024) 103206

with η spatio-temporal white noise, and $\varepsilon = 1/N$ for N random walkers. It can be interpreted as a functional gradient flow

$$\partial_t \rho = -M(\rho)\frac{\delta E[\rho]}{\delta \rho} + \sqrt{2\varepsilon} M_{1/2}(\rho)\eta \tag{5}$$

in the entropy landscape

$$E[\rho] = \int \rho \log \rho \, \mathrm{d}x$$

and with mobility operator

$$M(\rho)\xi = \nabla \cdot (\rho \nabla \xi) \tag{6}$$

(and thus $M_{1/2}(\rho)\xi = \nabla \cdot (\sqrt{\rho}\xi)$). The main point of this paper is to generalise the Eyring–Kramers formula (4) to generalised gradient systems (5) with conserved quantities.

1.1. Main result

The major problem in applying the Eyring–Kramers formula (4) to generalised gradient systems of the form (5) is that in almost all cases of physical relevance, the mobility operator is not positive definite, but instead features zero-eigenvalues corresponding to conserved quantities. For example the mobility in (6) has a zero eigenvalue, with constant functions being the corresponding eigenfunctions, that is associated with conservation of particle number for the underlying particle diffusion equation. This situation is generic in hydrodynamic limits, which often conserve mass, momentum, energy, etc. Our main result is a modification to the Eyring–Kramers formula, which corrects for the conserved quantity. For a single conserved quantity, it is given by

$$\tau = \frac{2\pi}{\mu_-}\sqrt{\frac{|\det H_s|}{\det H_-}}\sqrt{\frac{\hat{m}\cdot H_s^{-1}\hat{m}}{\hat{m}\cdot H_-^{-1}\hat{m}}}\mathrm{e}^{\Delta U/\varepsilon} \tag{7}$$

where $\hat{m}$ is the vector normal to the conserved quantity submanifold, and where stable fixed point x_- and saddle point x_s have to be appropriately re-interpreted. An extension to multiple conserved quantities will also be provided in section 2.3.

We remark that while a non-invertible mobility operator leads to divergences in the naive formula for the prefactor, a similar situation may also occur on the level of a diffusion without mobility, where the Hessian of the potential itself might be degenerate at the saddle point or at the fixed point, as discussed for example in [11, 16].

In the following, we will derive equation (7) via a formal asymptotic expansion. In particular, we will compute the asymptotics of the mean first passage time in section 2 through a boundary layer analysis and Laplace asymptotics, incorporating the complications of the conserved quantity. We will then demonstrate the applicability of the formula by computing mean first passage times for a simple toy model in section 3, and to two more realistic stochastic partial differential equations describing liquid thin film

J. Stat. Mech. (2024) 103206

rupture in section 4, and urban segregation in a socioeconomic model of social dynamics in section 5.

2. Mean first passage time and laplace asymptotics

In this section, we will derive equation (7) via a formal asymptotic expansion. We start with deriving a generic formula for a general stochastic differential equation and perform its boundary layer analysis in section 2.1. In section 2.2, we then specialize to the case of (non-degenerate) gradient flows with mobility (3) and apply Laplace asymptotics to derive the well-known case of the literature. Lastly, in section 2.3, we apply the same reasoning to the case at hand, namely gradient flows with degenerate mobility, where a conserved quantity yields a mobility matrix that is no longer positive definite. This chain of arguments yields our newly proposed formula, which we subsequently discuss in the context of stochastic hydrodynamics in section 2.4. While the original chain of arguments could be phrased in the more rigorous language of capacity theory as well, it is at this functional stage that a rigorous proof is much harder to achieve, and we thus resort to formal arguments throughout. We present our final full computational scheme in section 2.5 that forms the basis for our examples in sections 3–5.

Consider first the general stochastic differential equation for $X_t \in \mathbb{R}^n$,

$$\mathrm{d}X_t = b(X_t)\,\mathrm{d}t + \sqrt{\varepsilon}\sigma(X_t)\,\mathrm{d}W_t\,, \tag{8}$$

where $b : \mathbb{R}^n \to \mathbb{R}^n$ is the deterministic drift, $\sigma : \mathbb{R}^n \to \mathbb{R}^{n\times n}$ defines the noise covariance matrix $a(x) = \sigma(x)\sigma^T(x)$, and W_t is n-dimensional Brownian motion. We assume the case where there is a stable fixed point $x_- \in \mathbb{R}^n$ such that $b(x_-) = 0$ and the eigenvalues of $\nabla b(x_-)$ all have negative real part. We are interested in the time it takes the process to first exit the basin of attraction B of x_- starting at $x \in B$,

$$T_B(x) = \inf\{t > 0 \mid X_t \notin B\}\,.$$

$T_B(x)$ is a random variable, and its expectation $w_B(x) = \mathbb{E}T_B(x)$, the so-called *mean first passage time*, fulfills the inhomogeneous stationary Kolmogorov equation [17]

$$\begin{cases} \mathcal{L}w_B(x) = -1 & \text{for } x \in B \\ w_B(x) = 0 & \text{for } x \in \partial B\,, \end{cases} \tag{9}$$

where ∂B is the boundary of the basin of attraction of x_-, for which $\hat{n}\cdot b(u) = 0\ \forall\ u \in \partial B$, with $\hat{n}$ being the outwards pointing normal vector to ∂B. Here,

$$\mathcal{L} = b(x)\cdot\nabla + \tfrac{1}{2}\varepsilon a(x) : \nabla\nabla \tag{10}$$

is the generator of the SDE (8), from which we can deduce the invariant distribution $\rho_\infty(x)$ through the stationary Fokker–Planck equation

$$\mathcal{L}^\dagger\rho_\infty = 0\,,$$

where $\mathcal{L}^\dagger$ is the L^2-adjoint of the generator.

J. Stat. Mech. (2024) 103206

In the case of the gradient flow (3), the invariant distribution is given as Gibbs distribution through the potential itself,

$$\rho_\infty(x) = C\mathrm{e}^{-U(x)/\varepsilon}. \tag{11}$$

Further, there is a distinguished point x_s on ∂B for transitions from x_- out of B, given through the *barrier height* [11],

$$\Delta U = \inf_{u\in\partial B}(U(u) - U(x_-))$$

i.e. the smallest potential barrier encountered by continuous curves starting at x_- and leaving through ∂B. The point at which this barrier is taken, $x_s \in \mathbb{R}^n$, is assumed to be a saddle point with a single unstable direction, i.e. $\nabla U(x_s) = 0$ and $M(x_s)\nabla\nabla U(x_s)$ having exactly one negative eigenvalue μ_-, and $n-1$ positive eigenvalues. In general there might be multiple saddles, all of which are dominated by x_s, which is therefore called the *relevant saddle*. In the following, we write $M_s = M(x_s)$.

From large deviation theory [8] it is then known that

$$w_b(x_-) \asymp \mathrm{e}^{\varepsilon^{-1}(U(x_s)-U(x_-))}, \tag{12}$$

which determines the exponential part of the mean first passage time, recovering *Arrhenius' law* [7]. The purpose of the Eyring–Kramers law, and the goal of this paper, is to go beyond this mere exponential scaling law, and get sharp asymptotics of the prefactor omitted in (12).

2.1. Asymptotic expansion and boundary layer analysis

In order to get access to the prefactor, and loosely following [17], we assume $w_B(x) \asymp \mathrm{e}^{K/\varepsilon}$ as estimated by large deviation theory (12) and work with

$$\tau(x) = \mathrm{e}^{-K/\varepsilon} w_B(x),$$

which fulfills, via (9), the Kolmogorov equation

$$\begin{cases} \mathcal{L}\tau(x) = -\mathrm{e}^{-K/\varepsilon} & \text{for } x \in B \\ \tau(x) = 0 & \text{for } x \in \partial B, \end{cases}$$

so that for $\varepsilon \to 0$ the right hand side vanishes and the Kolmogorov equation becomes homogeneous. Since the diffusive term in the generator is $\mathcal{O}(\varepsilon)$ as well, we can assume that within B the variable $\tau(x)$ is merely advected and thus constant, $\tau(x) = C_0$, to leading order in ε. We need to consider only the behavior in a small $\mathcal{O}(\sqrt{\varepsilon})$ boundary layer near ∂B.

For a point x near the boundary ∂B, we choose coordinates

$$x = u - \sqrt{\varepsilon}\eta\hat{n},$$

for $\eta > 0$ and $u \in \partial B$, compare figure 1. In this boundary layer, to leading order, we therefore have

J. Stat. Mech. (2024) 103206

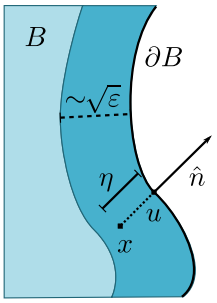

Figure 1. Schematic depiction of the boundary layer along ∂B: In an $\mathcal{O}(\sqrt{\varepsilon})$ vicinity, a point $x \in B$ is expanded along normal direction $\hat{n}$ from boundary point $u \in \partial B$, with local coordinate $\eta > 0$.

$$\mathcal{L} \approx (b(x)\cdot\hat{n})\frac{1}{\sqrt{\varepsilon}}\partial_\eta + \underbrace{\hat{n}\cdot a(x)\,\hat{n}}_{\alpha(u)}\partial_\eta^2 .$$

Since x is $\mathcal{O}(\sqrt{\varepsilon})$-close to $u \in \partial B$, we can expand

$$b(x)\cdot\hat{n} = \underbrace{b(u)\cdot\hat{n}}_{=0} + \hat{n}\cdot\nabla b(u)\,(x-u) + \mathcal{O}\left(|x-u|^2\right),$$

and introduce the additional quantity $\beta(u)$ through

$$\hat{n}\cdot\nabla b(u)\,(x-u) = -\sqrt{\varepsilon}\eta\underbrace{\hat{n}\cdot\nabla b(u)\,\hat{n}}_{\beta(u)} .$$

We will later see that $\beta(u)$ at the saddle $u = x_s$ is related to the unstable eigenvalue μ_-. Now, all terms are $\mathcal{O}(\varepsilon^0)$ and we arrive at

$$0 = \mathcal{L}\tau(\eta) = \eta\beta(u)\,\partial_\eta\tau(\eta) + \alpha(u)\,\partial_\eta^2\tau(\eta), \tag{13}$$

with α, β being the leading-order contributions of the normal terms of a and b, respectively. Equation (13) is solved by

$$\tau(\eta) = C_1(u)\int_0^\eta \mathrm{e}^{-\frac{\beta(u)}{2\alpha(u)}\eta^2}\,\mathrm{d}\eta .$$

Since we know the limit $\tau(\eta) \xrightarrow{\eta\gg 1} C_0$, we must have the matching condition

$$C_1(u) = C_0\sqrt{\frac{2\beta(u)}{\pi\alpha(u)}},$$

J. Stat. Mech. (2024) 103206

from which we can obtain C_0. The connection between the bulk and the boundary can be exploited when integrating $\mathcal{L}\tau(x) = -\mathrm{e}^{-K/\varepsilon}$ against the invariant density $\rho_\infty(x)$, and integrating by parts,

$$\begin{aligned}
-\mathrm{e}^{-K/\varepsilon}\int_B \rho_\infty(x)\,\mathrm{d}x &= \int_B \rho_\infty(x)\,\mathcal{L}\tau(x)\,\mathrm{d}x \\
&= \int_B \underbrace{\left(\mathcal{L}^\dagger\rho_\infty\right)}_{=0}\tau(x)\,\mathrm{d}x + \\
&\quad \int_{\partial B}\Bigg(\rho_\infty(\hat{n}\cdot b(u))\underbrace{\tau(u)}_{\tau=0\,\mathrm{on}\,\partial B} + \varepsilon\Big(\rho_\infty\hat{n}\cdot a(u)\nabla\tau(u) \\
&\quad - \underbrace{\tau(u)}_{\tau=0\,\mathrm{on}\,\partial B}\hat{n}\cdot a(u)\nabla\rho_\infty\Big)\Bigg)\,\mathrm{d}u \\
&= -\sqrt{\varepsilon}\int_{\partial B}\rho_\infty(u)\,\alpha(u)\,\partial_\eta\tau\,\mathrm{d}u \\
&= -\sqrt{\frac{2\varepsilon}{\pi}}C_0\int_{\partial B}\rho_\infty(u)\sqrt{\alpha(u)\,\beta(u)}\,\mathrm{d}u
\end{aligned}$$

so that

$$C_0 = \mathrm{e}^{-K/\varepsilon}\sqrt{\frac{\pi}{2\varepsilon}}\frac{\int_B\rho_\infty(x)\,\mathrm{d}x}{\int_{\partial B}\rho_\infty(u)\sqrt{\alpha(u)\,\beta(u)}\,\mathrm{d}u}.$$

We conclude that in the interior,

$$w_B(x_-) = \sqrt{\frac{\pi}{2\varepsilon}}\frac{\int_B\rho_\infty(x)\,\mathrm{d}x}{\int_{\partial B}\rho_\infty(u)\sqrt{\alpha(u)\,\beta(u)}\,\mathrm{d}u}. \tag{14}$$

2.2. Laplace asymptotics

Note that so far we have not made use of the fact that our system is a gradient flow with non-degenerate mobility (3), and that result (14) is asymptotically correct for $\varepsilon \ll 1$ for arbitrary systems. We can now make use of our explicit knowledge of the invariant measure (11) to apply Laplace asymptotics to the volume and boundary integrals in (14). Concretely, that means that in the numerator, we can approximate

$$\int_B\rho_\infty(x)\,\mathrm{d}x \approx \frac{(2\pi\varepsilon)^{n/2}}{\sqrt{\det H_-}}\mathrm{e}^{-U(x_-)/\varepsilon},$$

since x_- is the minimum of U within B, while in the denominator

$$\int_{\partial B}\rho_\infty(u)\sqrt{\alpha(u)\,\beta(u)}\,\mathrm{d}u \approx \frac{(2\pi\varepsilon)^{(n-1)/2}}{\sqrt{|\det H_s|}}\sqrt{\alpha(s)\,\beta(s)}\left(\hat{n}\cdot H_s^{-1}\hat{n}\right)^{-1/2}\mathrm{e}^{-U(x_s)/\varepsilon},$$

J. Stat. Mech. (2024) 103206

where the $(\hat{n}\cdot H_s^{-1}\hat{n})$-term comes from the fact that we integrate the Gaussian integral only over the tangent space to the separatrix at the saddle, $T_{x_s}\partial B$, as derived in the appendix in lemma 4. In total, this yields

$$w_B(x_-) = \pi\sqrt{\frac{\hat{n}\cdot H_s^{-1}\hat{n}}{\alpha(x_s)\,\beta(x_s)}}\sqrt{\frac{|\det H_s|}{\det H_-}}\mathrm{e}^{\Delta U/\varepsilon},$$

where we recall that $\alpha(x_s)=\hat{n}\cdot M_s\hat{n}$ and $\beta(x_s)=\hat{n}\cdot M_sH_s\hat{n}$, and where the $\mathcal{O}(\varepsilon)$-part of the drift term $b(x)=-M(x)\nabla U(x)+\varepsilon\nabla\cdot M(x)$ is subdominant and thus dropped. Here we write $M(x_s)=M_s$, $\nabla\nabla U(x_-)=H_-$ and $\nabla\nabla U(x_s)=H_s$.

Using lemmas 2 and 3 of the appendix, we recognise that $\alpha(x_s)$ and $\beta(x_s)$ are connected to μ_- via

$$\beta(x_s)=\frac{\alpha(x_s)}{\hat{n}\cdot H_s^{-1}\hat{n}}=\mu_-\,,$$

where μ_- is the unique negative eigenvalue of M_sH_s. We arrive at the final result

$$w_B(x_-)=\frac{\pi}{\mu_-}\sqrt{\frac{|\det H_s|}{\det H_-}}\mathrm{e}^{\Delta U/\varepsilon}.$$

This demonstrates the capacity theory result from the literature [13] for the case of gradient flows with position-dependent mobility.

2.3. Conserved quantities of the mobility matrix

We now consider the case where the system has a conserved quantity, understood in the sense that the mobility matrix $M(x):\mathbb{R}^n\to\mathbb{R}^{n\times n}$ is no longer positive definite, but positive semi-definite. In other words, for each $x\in\mathbb{R}^n$, there exists a number of zero eigenvalues of $M(x)$, and $M(x)$ is no longer full rank. As a consequence, since the mobility acts in front of both the deterministic drift and the stochastic noise, the degrees of freedom associated with the zero eigenvalues are never changed, and remain a constant of integration. The concrete value of the conserved quantity and their nature depends on both the mobility matrix and the initial condition of the system.

For simplicity, we consider a single conserved quantity, so that $M(x)$ has a unique zero eigenvalue for all $x\in\mathbb{R}^n$ with normalised eigenvector $\hat{m}(x)$, while all its other eigenvalues are strictly positive. The process (3) then remains constrained to an $(n-1)$-dimensional sub-manifold $S\subset\mathbb{R}^n$, with normal vector field $\hat{m}(x)$, since neither the gradient drift nor the stochastic force can ever have a contribution in the direction of $\hat{m}$.

This situation is depicted in figure 2. Note that, while the original fixed points (both stable, $y_\pm$, and saddle y_s) of the system still exist, they do not lie within S. Instead, the effective stable points x_+ and x_- that should be considered for the Laplace asymptotics are no longer (local) minima of the potential $U(x)$, but instead are only

J. Stat. Mech. (2024) 103206

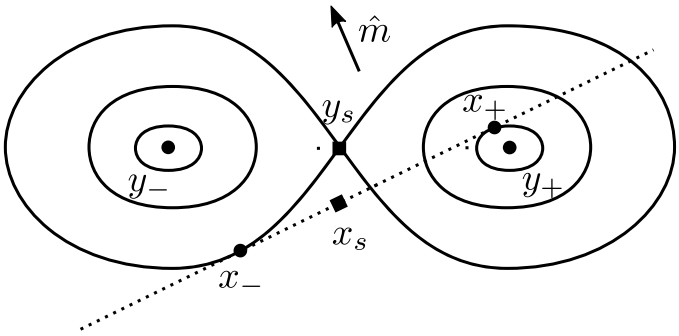

Figure 2. Conserved quantities of the stochastic process: If $M(x)$ has a zero eigenvalue with eigenvector $\hat{m}$, then the gradient diffusion (3) will remain constrained to a submanifold $S \in \mathbb{R}^n$ (dotted line) with normal vector $\hat{m}$. Instead of the actual fixpoints $\{y_-, y_s, y_+\}$, the relevant points are now the corresponding fixed points $\{x_-, x_s, x_+\}$ of the dynamics constrained to the submanifold S.

local minima of the potential constrained to the submanifold S, so that $\nabla U(x_-) \parallel \hat{m}$ instead of $\nabla U(x_-) = 0$. The same is true for the effective saddle point x_s, which is no longer a proper saddle of $U(x)$. Therefore, the new basin of attraction, $\tilde{B}$, is now a subset of S instead of all of $\mathbb{R}^n$, as is its boundary, $\partial\tilde{B}$. As before, we write $M_s := M(x_s)$, $H_s = \nabla\nabla U(x_s)$ and $H_- = \nabla\nabla U(x_-)$.

In fact, all arguments made in sections 2.1 and 2.2 go through with the minor modification of operating in the $(n-1)$-dimensional tangent spaces $T_{x_-}S$ and $T_{x_s}S$ around the stable point and the saddle instead of all of $\mathbb{R}^n$. This is possible in particular because at the saddle point x_s, the space of conserved quantities $T_{x_s}S$ cannot be parallel to the separatrix ∂B, or in other words $\hat{n}(x_s) \nparallel \hat{m}(x_s)$ (where we recall that $M_s\hat{m}(x_s) = 0$ and $H_s M_s \hat{n}(x_s) = \mu^+$). In fact, as shown in lemma 6, $\hat{n}$ and $\hat{m}$ are perpendicular in the H_s^{-1} inner product, which simplifies the integration. Following similar arguments in section 2.1 one can derived the mean first passage time with a conserved quantity to be

$$w_B(x_-) = \sqrt{\frac{\pi}{2\varepsilon}} \frac{\int_{\tilde{B}} \rho_\infty(x)\,\mathrm{d}x}{\int_{\partial\tilde{B}} \rho_\infty(u)\sqrt{\alpha(u)\,\beta(u)}\,\mathrm{d}u}. \tag{15}$$

The volume and boundary integrals in (15) can be evaluated using the invariant measure (11) and the Laplace approximation as in section 2.2. Note that additional correcting factors need to be introduced when we apply the Laplace method and integrate over $\tilde{B} \subset S$ and $\partial\tilde{B}$, as shown by lemmas 4 and 5 in the appendix. In particular, we get

$$\begin{aligned}\int_{\tilde{B}} \rho_\infty(x)\,\mathrm{d}x &= \int_{\tilde{B}} \mathrm{e}^{-U(x)/\varepsilon}\,\mathrm{d}x \overset{\varepsilon\to 0}{=} \mathrm{e}^{-U(x_-)/\varepsilon} \int_{T_{x_-}\tilde{B}} \mathrm{e}^{-\frac{1}{2}x\cdot H_- x}\,\mathrm{d}x \\ &= \sqrt{\frac{(2\pi\varepsilon)^{n-1}}{\det H_-}} \left|\hat{m}\cdot H_-^{-1}\hat{m}\right|^{-1/2} \mathrm{e}^{-U(x_-)/\varepsilon}\end{aligned}$$

J. Stat. Mech. (2024) 103206

at the stable fixed point, and

$$\begin{aligned}\int_{\partial\tilde{B}} \sqrt{\alpha(u)\beta(u)}\rho_\infty(u)\,\mathrm{d}u &= \int_{\partial\tilde{B}} \sqrt{\alpha(u)\beta(u)}\mathrm{e}^{-U(u)/\varepsilon}\,\mathrm{d}u \\ &\overset{\varepsilon\to 0}{=} \sqrt{\alpha(x_s)\beta(x_s)}\mathrm{e}^{-U(x_s)/\varepsilon}\int_{T_{x_s}\partial\tilde{B}} \mathrm{e}^{-\frac{1}{2}u\cdot H_s u}\,\mathrm{d}u \\ &= \sqrt{\frac{(2\pi\varepsilon)^{n-2}}{\det H_-}}\frac{\sqrt{\alpha(x_s)\beta(x_s)}}{|\hat{m}\cdot H_s^{-1}\hat{m}|^{1/2}\,|\hat{n}\cdot H_s^{-1}\hat{n}|^{1/2}}\mathrm{e}^{-U(x_s)/\varepsilon}\end{aligned}$$

at the saddle point. Recall $\alpha(x_s)=\hat{n}\cdot M_s\hat{n}$, $\beta(x_s)=\hat{n}\cdot M_s H_s\hat{n}$, and using lemmas 2 and 3 of the appendix, we arrive at our final result

$$\tau = \frac{2\pi}{\mu_-}\sqrt{\frac{|\det H_s|}{\det H_-}}\sqrt{\frac{\hat{m}\cdot H_s^{-1}\hat{m}}{\hat{m}\cdot H_-^{-1}\hat{m}}}\,\mathrm{e}^{\Delta U/\varepsilon}, \tag{16}$$

where we additionally used the fact that the expected time of transitions τ is twice the expected time to exit, $w_B(x_-)$.

Remark 1. If we define as $A\big|_V$ the restriction of an operator $A:\mathbb{R}^n\to\mathbb{R}^n$ to a subspace $V\subset\mathbb{R}^n$, i.e. $A\big|_V : V\to\mathbb{R}^n$, then equation (16) can be equivalently written via determinants of the Hessians restricted to the tangent spaces of the conserved manifold at the two relevant points,

$$\tau = \frac{2\pi}{\mu_-}\sqrt{\frac{\left|\det\left(H_s\big|_{T_{x_s}S}\right)\right|}{\det\left(H_-\big|_{T_{x_-}S}\right)}}\,\mathrm{e}^{\Delta U/\varepsilon}. \tag{17}$$

While notationally more pleasing, this formulation is less readily implementable numerically, as it necessitates finding a basis for the tangent spaces and expressing the Hessians in this basis, while equation (16) simply corrects for the single conserved quantity under knowledge of the vector $\hat{m}$.

Remark 2. Via a repeated application of our arguments (see lemma 7), one can generalize equation (16) to multiple conserved quantities by choosing an appropriate basis for the space of conserved quantities. Concretely, for vectors $\{\hat{m}_1,\ldots,\hat{m}_k\}$ normal to the conserved manifold S, under the assumption that m_i are orthogonal in the H^{-1} inner product, we obtain

$$\tau = \frac{2\pi}{\mu_-}\sqrt{\frac{|\det H_s|}{\det H_-}}\sqrt{\frac{\hat{m}_1\cdot H_s^{-1}\hat{m}_1}{\hat{m}_1\cdot H_-^{-1}\hat{m}_1}}\cdots\sqrt{\frac{\hat{m}_k\cdot H_s^{-1}\hat{m}_k}{\hat{m}_k\cdot H_-^{-1}\hat{m}_k}}\,\mathrm{e}^{\Delta U/\varepsilon}.$$

The variant via restricted Hessians, equation (17), remains unchanged in this case.

Remark 3. Of course it might be simpler, in particular in finite dimensional systems, to consider instead of the original stochastic evolution equation a reduced equation that eliminates variables to enforce the conservation constraint explicitly. For example, for a

J. Stat. Mech. (2024) 103206

chemical reaction transforming molecule A into B and back, but with the total number $A+B$ conserved, one could instead consider stochastic dynamics in the difference $A-B$. While sometimes this approach is practical, and it must lead to identical results, it often produces complicated equations, in particular in the functional setting.

2.4. Functional gradient flows and stochastic hydrodynamics

While the above discussion and derivation focuses on gradient flows in $\mathbb{R}^n$, following the work in [15], it has been realised that a vast array of systems that originate from macroscopic limits of microscopic interacting particle systems can similarly be interpreted as gradient flows, on the space of probability measures, and as generalised Wasserstein-gradient flows of an entropy functional. The easiest example is the many-particle limit of non-interacting Brownian walkers, in the large particle limit, $N\to\infty$, but interactions with external forces, surrounding fluids, or inter-particle interactions can be incorporated as well. For finite but large number of particles, $N\gg 1$, one expects fluctuations of the order $1/\sqrt{N}$ and arrives at a *stochastic* evolution equation in the form of a stochastic partial differential equation (SPDE), generally summarised under the notion of *fluctuating hydrodynamics* [18–20]. If the underlying microscopic model is in detailed balance, so is the resulting stochastic hydrodynamics equation. For the example of $N=1/\varepsilon$ non-interacting random walkers,

$$\mathrm{d}X_i(t)=\sqrt{2D}\mathrm{d}W_i(t)\,,$$

the limiting SPDE for the density $\rho(x,t)$ of walkers is formally given by

$$\partial_t\rho(x,t)=D\Delta\rho(x,t)+\sqrt{2D\varepsilon}\partial_x\left(\sqrt{\rho(x,t)}\eta(x,t)\right),$$

which is a functional gradient flow

$$\partial_t\rho=-M(\rho)\frac{\delta E[\rho]}{\delta\rho}+\sqrt{2\varepsilon}M_{1/2}(\rho)\eta\,,$$

with

$$E[\rho]=\int\rho\log\rho\,\mathrm{d}x\,,\quad\text{and}\quad M(\rho)\xi=D\nabla\cdot(\rho\nabla\xi)\,.$$

The above limiting equation is formal, and there is considerable effort involved in making this intuition rigorous, in particular for nonlinear equations and in higher dimensions. The precise mathematical interpretation of the resulting SPDEs is subject to active research [21, 22]. This includes, but is not limited to, the interpretation of the $\mathcal{O}(\varepsilon)$-divergence term in (3), which for many nonlinear equations diverges and requires renormalization. For the purposes of this paper, we retreat to the notion that ultimately, every numerical computation relies on discretization and hence an 'UV' cutoff that regularises any divergences. In systems of physical meaning, such a cut-off can be naturally

J. Stat. Mech. (2024) 103206

justified as length scale where the continuum limit breaks down, such as the size of a molecule for a fluid. In this sense, any spatially continuous SPDE is to be interpreted as a notational shorthand for a discrete system with an appropriate physical cut-off length scale.

2.5. Full computational scheme

Given the above derivation, we now have a complete recipe for computing mean first passage times for metastable stochastic hydrodynamics. Concretely, in order to estimate the mean first passage time out of a locally stable configuration, we apply the following steps:

(i) Compute the saddle point (for example via edge tracking or gentlest ascent dynamics (GAD) [23]) constrained to the submanifold restriction, respecting the conserved quantities.
(ii) Compute the Hessian around the effective saddle and stable fixed point by discretizing the continuous operator via some spatial discretization scheme.
(iii) Compute the spectrum of this Hessian, and correct for its action in conserved normal direction (the subspace perpendicular to mass conservation).

The result will be a quantitative estimate for the mean first passage time for the small noise limit. Notably, there is no fitting parameter or additional assumption. The computation has to be done only once, and can then be used for any noise strength ε (but of course will be more accurate for smaller ε).

In the following section, we will demonstrate the applicability of this scheme to a number of examples, starting with a two-dimensional and easy to visualise toy example in section 3, and then two stochastic partial differential equations motivated from interacting particle systems and stochastic hydrodynamics: the rupture time for liquid thin films in section 4, and the a socio-economic model of urban separation in section 5.

3. Two-dimensional gradient flow

As a simple and easy to visualise example, we first consider a double-well for $(x,y) \in \mathbb{R}^2$ given by

$$U(x,y) = \tfrac{1}{4}\left(1-x^2\right)^2 + \tfrac{1}{2}y^2\left(x^2+\tfrac{1}{4}\right). \tag{18}$$

While this potential has two minima, at $(-1,0)$ and $(1,0)$, and a saddle at $(0,0)$, we want to modify the gradient flow with the mobility matrix

$$M(x,y) = \tfrac{1}{2}\left(1+x^2\right)\hat{p}\hat{p}^T,$$

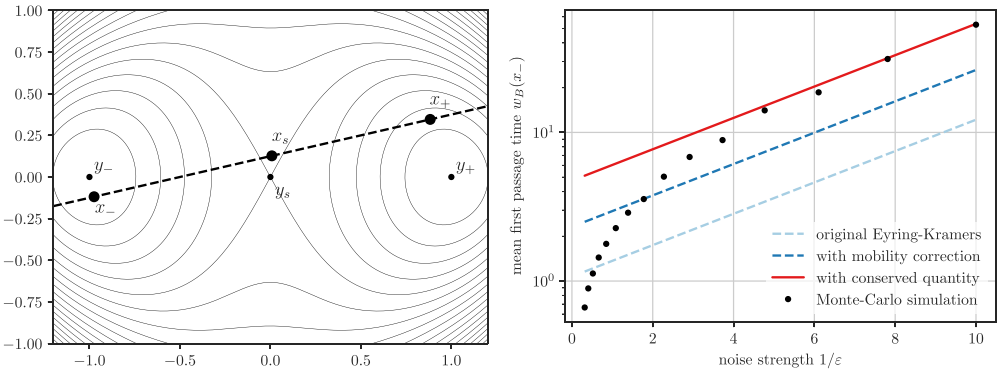

Figure 3. Left: Doublewell (18) with conserved quantity. While the full double-well, with minima $y_\pm$ and saddle y_s, adheres to the original Eyring–Kramers formula (4), the actual system (19) has a conserved quantity, restricting it to the dashed subspace. Not only does this result in different minima $x_\pm$ and saddle x_s of the restricted system, but the ratio of Hessians in the Eyring–Kramers formula becomes incorrect, as it considers curvatures into suppressed directions. Right: Time to leave the basin of attraction of x_- as a function of the noise amplitude ε. Dots show the result of 1000 numerical simulations of (19) each, compared to the original Eyring–Kramers formula (2) (light blue dashed), the formula (4) taking into account the mobility matrix (dark blue dashed), and finally our formula (16) further taking into account the conserved quantities (red solid). Clearly, both corrections are needed to explain the observed times.

for a normalised vector $\hat{p} \in \mathbb{R}^2$. Since $M(x)$ has a zero eigenvalue with corresponding eigenvector $\hat{m} = (\hat{p})^\perp$, the gradient flow

$$\mathrm{d}\left(X_t, Y_t\right) = -M\left(X_t, Y_t\right) \nabla U\left(X_t, Y_t\right) \mathrm{d}t + \varepsilon \nabla \cdot M\left(X_t, Y_t\right) + \sqrt{2\varepsilon} M_{1/2}\left(X_t, Y_t\right) \left(\mathrm{d}W_x, \mathrm{d}W_y\right) \tag{19}$$

will always remain confined to the subspace

$$S = \left\{(x, y) \in \mathbb{R}^2 \middle| \ \begin{pmatrix} x & y \end{pmatrix} \cdot \hat{m} = k \right\}.$$

In other words, the quantity $k = \begin{pmatrix} x & y \end{pmatrix} \cdot \hat{m}$ is a conserved quantity of equation (19), similar to how mass is conserved in fluctuating hydrodynamic equations. Its value throughout remains that of the initial conditions of (19). This situation is depicted in figure 3(left).

For a numerical experiment to demonstrate the correctness of our formula, we concretely pick $p = (1, \frac{1}{4})$ and $\hat{p} = p/|p|$, and initialise with the conserved quantity set to $k = \frac{1}{8}$. With these values, we can numerically measure the mean time it takes to exit the basin of attraction of the left well, and compare the results to our formula in section 2. The equation (19) is solved using a fourth order Runge–Kutta method [24]

J. Stat. Mech. (2024) 103206

with timestep $\mathrm{d}t = 5 \cdot 10^{-3}$. Figure 3(right) shows the results of the Monte-Carlo experiment, simulating $N = 1000$ samples for each value of ε and averaging the observed time to exit the basin of attraction of the left well. This is compared against the original Eyring–Kramers formula (2) considering only the properties of the Hessian (light blue dashed), the generalised Eyring–Kramers formula including the correction from the mobility operator, equation (4) (dark blue dashed), and lastly our final result (16) which further considers the correction of the restriction to the conserved subspace. As can be seen, the change of eigenvalue from λ_- to μ_-, as well as the conserved quantity correcting factor $\sqrt{(\hat{m} \cdot H_s^{-1}\hat{m})/(\hat{m} \cdot H_-^{-1}\hat{m})}$, both lead to a correcting factor of roughly 2, and both corrections are needed in order to explain the observed result. We stress that in order to obtain the fully corrected Eyring–Kramers law (16), a single computation needs to be done for a prediction for all ε, and without any fitting parameter. The small noise limit, $\varepsilon \ll 1$, appears to work reasonably well already for values $\varepsilon < \frac{1}{4}$.

4. Stochastic hydrodynamics and thin film rupture

The stability of nanoscale thin liquid films on solid substrates plays a key role in many applications including coating [25], nanofluidic transistors [26] and nanomanufacturing [27]. It has been observed both experimentally [28–30] and numerically with molecular dynamics simulations [31–33] that initially flat films would rupture spontaneously, as shown in figure 4(left). The classical explanation for the rupture is due to the competition between the disjoining pressure (otherwise known as the van der Waals forces) and the surface tension, and a linear stability analysis [34] further reveals a critical wavelength above which the wave modes are linearly unstable, eventually leading to rupture. However, subsequent observations [30] have revealed a larger set of regimes, one of which was hypothesised to stem from *thermally* activated rupture in the linearly stable regime.

Nanoscale films are difficult to observe experimentally and often molecular dynamics is utilised to explore their stability. However, MD can be computationally expensive, and thus there has been a drive towards developing macroscopic models to model this system. It has been observed [35, 36] that the evolution of the thin film follows a stochastic hydrodynamic limit, namely the stochastic thin film equation (STF) which, in the two-dimensional case, after non-dimensionalisation [33] reads

$$\partial_t h\,(x,t) = \partial_x \left[c\,(h)\,\partial_x \left(-\partial_x^2 h + \frac{4\pi^2}{3h^3} \right) + \sqrt{2\varepsilon c\,(h)}\eta \right]. \tag{20}$$

Here, $h(x,t)$ is the height of the thin film, $c(h) = h^3$ is the mobility associated with a no-slip solid, ε is the noise amplitude and η is a Gaussian white noise uncorrelated in both time and space, i.e. $\langle \eta(x,t)\eta(x',t') \rangle = \delta(x-x')\delta(t-t')$ where $\langle\,\rangle$ is the ensemble average and $\delta(x)$ is the Dirac delta functional. The STF is assumed to be periodic on $x \in [0,1]$ and the non-dimensionalisation is chosen so that the linear stability depends

J. Stat. Mech. (2024) 103206

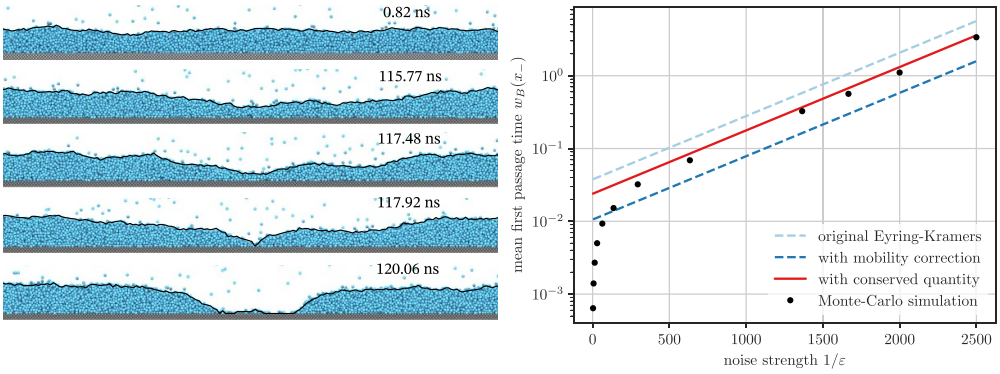

Figure 4. Left: Snapshots from molecular dynamics simulation of a thin liquid film on a solid substrate. The blue particles indicate liquid and vapor. The silver particles indicate solid. The black lines show the position of the liquid–vapor interface, i.e. the film height. While the film is initially flat, is eventually ruptures by thermal fluctuations. Right: Average waiting time for rupture of thin film is plotted as a function of the inverse strength of the fluctuations. As ε decreases, the observed average rupture time collapse onto the Eyring–Kramers prediction with our expression for the prefactor (16).

solely on the average film height $h_0 = \int_0^1 h(x,t)\mathrm{d}x = \text{const}$: for $h_0 > 1$ the film is linearly stable and small perturbations without thermal fluctuations would decrease exponentially with time. For simplicity we use a constant mobility $c(h) = h_0^3$. The STF can also be interpreted as a functional gradient flow

$$\partial_t h\,(x,t) = -M\,(h)\,\frac{\delta E}{\delta h} + \sqrt{2\varepsilon} M_{1/2}\,(h)\,\eta\,,$$

for an energy functional

$$E\,[h] = \int_0^1 \left(\frac{1}{2}\,(\partial_x h)^2 - \frac{2\pi^2}{3h^2}\right)\mathrm{d}x\,, \tag{21}$$

with mobility operator (acting on a test-function $\xi(x)$)

$$M\,(h)\,\xi = -\partial_x\left(h_0^3 \partial_x \xi\right)\,,$$

and

$$M_{1/2}\,(h)\,\xi = \sqrt{h_0^3}\,\partial_x \xi\,.$$

The thermally activated rupture of the liquid nanofilm can then be interpreted as a diffusive exit of the SPDE (20) from the basin of attraction of the spatially constant solution

$$h\,(x,t) = h_0 > 1\,.$$

J. Stat. Mech. (2024) 103206

Additionally, the system obeys mass conservation, and as such constant functions are a zeromode of the mobility operator. Therefore, in order to compute the expected time to rupture, our full formalism (16) is necessary. Specifically, the computation consists of the following steps: (1) we compute the saddle point of the energy functional (21) via GAD, (2) we compute the second variation of the energy functional, acting on a test function $\xi(x)$ at an arbitrary point h^*, given by (see appendix B)

$$\frac{\delta^2 E\left[h\left(x\right)\right]}{\delta h\left(x\right)^2}\Big|_{h=h^*}\xi\left(x\right) = -\frac{4\pi^2}{h^*\left(x\right)^4}\xi\left(x\right) - \partial_x^2\xi\left(x\right),$$

and compute numerically the spectrum of this operator at the fixed point, $h^* = h_0$, and at the saddle, $h^* = h_s(x)$. The ratio of these Hessians, evaluated according to equation (2), yields the light blue dashed line in figure 4. (3) Since the mobility operator is not the identity, there is a correcting factor including μ_-, which we obtain numerically by computing the unique negative eigenvalue of the operator

$$M\left(h_s\left(x\right)\right)\frac{\delta^2 E\left[h\right]}{\delta h^2}\Big|_{h=h_s}\xi = h_0^3\partial_x^2\left[\left(\frac{4\pi^2}{h_s\left(x\right)^4} + \partial_x^2\right)\xi\right],$$

which yields instead the dark blue dashed line in figure 4. Lastly, we need to compute the action of the Hessian in direction of the vector normal to the conserved submanifold, which in this case is just the constant function $1(x) \equiv 1$. The inverse of the Hessian operator is evaluated numerically, and the result is the red solid line in figure 4, which agrees very well with the waiting time to rupture obtained via many stochastic Monte-Carlo experiments that integrate the STF equation (20) until a rupture is observed (black dots). The exponential time differencing method [37] is used for the Monte-Carlo experiments with timestep $\mathrm{d}t = 1.566 \cdot 10^{-7}$, and the details of implementation can be found in [33]. Here we choose the average film height to be $h_0 = 1.01$, the STF is solved on a domain with 128 uniformly distributed grid points, and the rupture times are averaged over 100 events. Note that in [33], additional molecular dynamics simulations demonstrated agreement of expected rupture times with equation (16).

To further characterise the rupture process, we investigate how the energy (21) changes with time near rupture. We perform 200 independent simulations and record the film profiles for $5 \cdot 10^5$ timesteps before the rupture time t_r. The energy is then calculated with the averaged profile to filter out the effect of thermal fluctuations, as shown in figure 5. The light blue lines and the black dashed line in the inset show the averaged profiles at different times and the analytical saddle shape calculated from GAD, respectively. It is shown that the energy increase as the averaged profile deviates from its flat steady state, until the averaged profile reaches the saddle shape h_s and drops dramatically. The analytical energy barrier is recovered from the simulations, and the analytical saddle shape agrees well with the averaged profile with maximum energy. These findings indicate that our saddle shape calculation is correct and the transition (or rupture) indeed goes through the saddle.

J. Stat. Mech. (2024) 103206

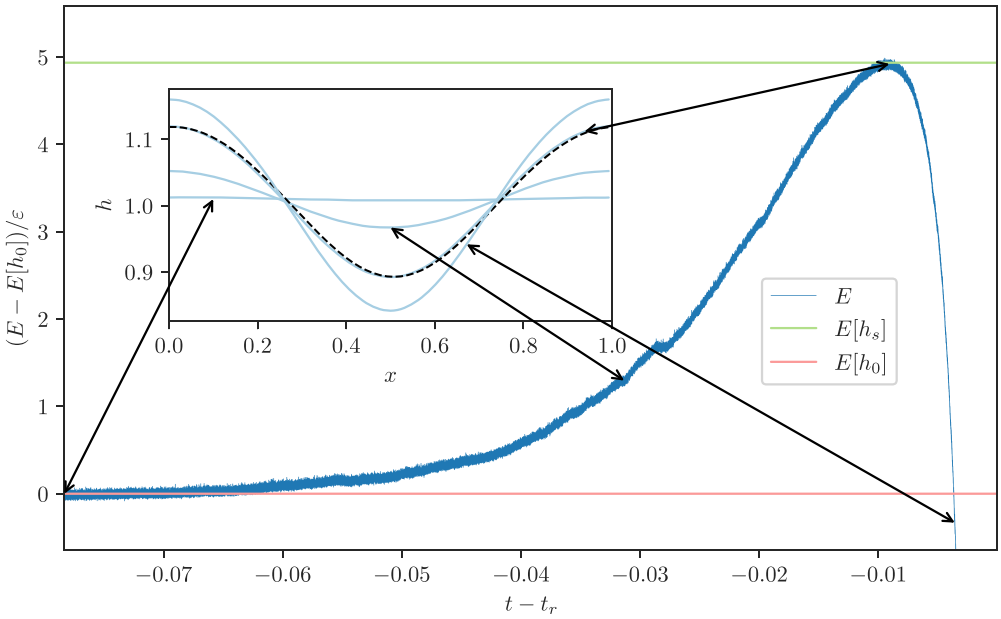

Figure 5. Change of energy near rupture time. Noise amplitude is choosen to be $\varepsilon = 0.0005$. The dark blue line is the energy of the averaged profile, the light red line is the energy of the flat profile and the light green line is the energy of the saddle shape calculated analytically via GAD. The energy is translated by the energy of the flat profile and normalised by noise amplitude ε. The inset shows the averaged profile at different times with light blue lines and the analytical saddle shape with black dashed lines.

5. Social dynamics and urban segregation

Fluctuating hydrodynamics SPDEs are not only encountered in continuum limits of actual fluid models, but are regularly derived whenever there is a large number of interacting agents, such as interacting active particles [38], in traffic flow [39], pedestrian dynamics [40, 41] and socioeconomic interactions [42]. In each case, the particles are replaced by agents capable of acting according to some simple ruleset. In socioeconomic models, a generic assumption is that the agents try to individualistically improve their own outcome or utility. In this context, the number of possible equilibrium states of the overall model, as well as their relative likelihood, becomes extremely important, as it describes directly the most likely emergent state that the system will spontaneously converge to. Consequently, the convergence to the ultimate stable state can be seen as the manifestation of the 'invisible hand' crystallizing the collective societal state out of the individual agents' behavior.

A well-known example is the phenomenon of urban segregation, described by the Schelling or Sakoda–Schelling models [43, 44]. In these, a large number of agents is prescribed, each belonging to one of multiple distinct sub-populations, for example representing social or ethnic background, which are free to relocate depending on their preferences. In the original model, the presence of only a slight preference of agents

J. Stat. Mech. (2024) 103206

to surround themselves with neighbors of their own sub-population led to completely segregated geographical regions in the long-time limit. Following ideas introduced in [42, 45, 46], these models can be simplified to consist only of a single population, with spatial exclusion and density dependent diffusivity, leading to a fluctuating hydrodynamic equation of

$$\partial_t \rho = \nabla \cdot \left((1-\rho) \nabla \left(D(\rho) \rho \right) + \rho D(\rho) \nabla \rho \right) + \nabla \cdot \left(\sqrt{\rho(1-\rho)} \eta(x,t) \right), \tag{22}$$

where η is spatio-temporally white noise and the diffusivity of agents is given by

$$D(\rho) = D_0 \mathrm{e}^{-CK\star\rho}. \tag{23}$$

This diffusivity exhibits a spatial convolution '$\star$' with a kernel K, representing non-local sensing of their neighborhood by each of the agents. In essence, equation (22) describes the (nonlinear) diffusion of agents under spatial exclusion, such that the density remains between 0 and 1, representing complete absence of agents to full occupation. The density dependent diffusivity (23) represents the tendency of agents to relocate towards a higher density of peers in the vicinity, up to some maximum range given by a spatial cutoff of the (symmetric) kernel $K(x,y) = K(x-y)$. This corresponds to energy and mobility given by

$$\begin{cases} E[\rho] = \int \left(\rho \log \rho + (1-\rho) \log(1-\rho) - \frac{1}{2} C \rho K \star \rho \right) \mathrm{d}x \\ M(\rho)\xi = -\nabla \cdot \left(\rho(1-\rho) D(\rho) \nabla \xi \right), \\ M_{1/2}(\rho)\xi = \nabla \cdot \left(\sqrt{\rho(1-\rho) D(\rho)} \xi \right), \end{cases} \tag{24}$$

where the mobility again conserves total mass, and we are in the framework where our results apply.

For simplicity, we assume the population density ρ is periodic on domain $x \in [0,1]$. We also assume a Gaussian kernel $K(z) = \frac{1}{\sqrt{2\pi}\kappa} \exp(-\frac{1}{2} z^2/\kappa^2)$ with sensing length scale $\kappa > 0$, corresponding to $\hat{K}(k) = \exp(-k^2\kappa^2/2)$ in Fourier space. Expanding the convolution for $\kappa \ll 1$ yields (see appendix C)

$$(K \star \rho)(x) = \rho(x) + \frac{\kappa^2}{2} \partial_x^2 \rho(x) + \mathcal{O}\left(\kappa^4\right).$$

The Hessian operating on a periodic test function $\xi(x)$ can then be expressed by (see appendix B)

$$\frac{\delta^2 E[\rho(x)]}{\delta \rho(x)^2} \xi(x) = \left(\frac{1}{\rho(x)} + \frac{1}{1-\rho(x)} - C \right) \xi(x) - \frac{\kappa^2}{2} C \partial_x^2 \xi(x).$$

For simplicity, we further assume that the population density is constant in the mobility operator, $\rho(x) = \bar{\rho}$, where $\bar{\rho} = \int_0^1 \rho \mathrm{d}x$ is the mass that is conserved. We can then calculate μ_- by numerically computing the unique negative eigenvalue of the operator

$$M(\bar{\rho}) \frac{\delta^2 E[\rho]}{\delta \rho^2} \xi = -\bar{\rho}(1-\bar{\rho}) D(\bar{\rho}) \partial_x^2 \left[\left(\frac{1}{\rho} + \frac{1}{1-\rho} - C - \frac{\kappa^2}{2} C \partial_x^2 \right) \xi \right].$$

J. Stat. Mech. (2024) 103206

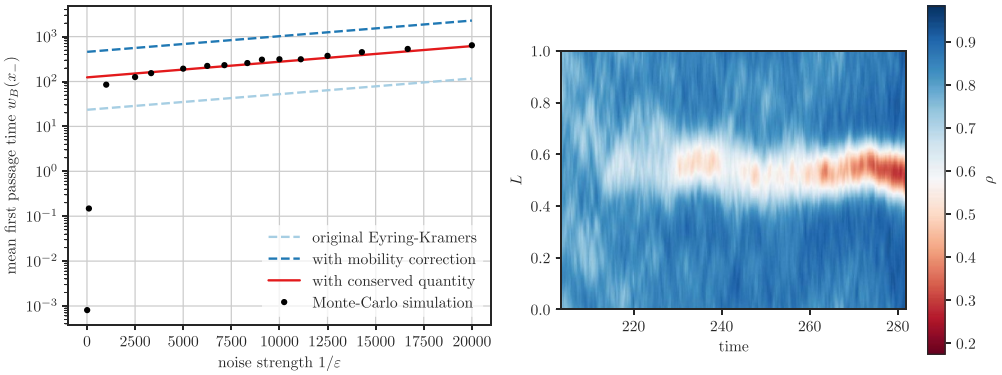

Figure 6. Left: average waiting time for the spontaneous segregation of the social dynamics model as a function of the inverse strength of fluctuations. After a transient for large noise, waiting times are exponentially distributed. The correct exponential distribution is correctly predicted, including its prefactor, by our formula (16), while naive application of the Eyring–Kramers formula leads to mispredictions of a factor 5. Right: evolution (time-space) of the density of agents near an observed segregation event. The originally homogeneous and fluctuating distribution of agents spontaneously segregates into a dense and a diluted region.

For the parameter $C = 6, \kappa = 8 \cdot 10^{-3}$, $D_0 = 1$ and mass $\bar{\rho} = \int \rho \mathrm{d}x = 0.7908$, this system exhibits multiple stable fixed points: A spatially homogeneous solution $\rho(x) = \bar{\rho}$, as well as a localised ('cluster' or 'aggregated') state with minimum $\rho_{\min} = 0.1747$, which observes an aggregation of the agents in part of the domain, leaving behind a depleted region where the concentration of agents is low. Both of these states are locally stable and hence long lived for small enough fluctuations. Fluctuations are understood to be spontaneous local movements of agents, preserving their total number, but rearranging them locally in space, with probabilities based both on the local densities (through the exclusion terms proportional to $\rho(1-\rho)$, which prevents movement out of empty or into fully occupied regions), as well as their perceived relative attractiveness encoded in the energy functional. As a result, an initially homogeneous population will eventually spontaneously segregate due to fluctuations. Population density ρ is discretised with 64 uniformly distributed grid points. Equation (22) is solved numerically using the same exponential time difference scheme as in the previous section with timestep $\mathrm{d}t = 7.832 \cdot 10^{-5}$. The population density is segregated when its minimum has reached $\rho_{\min}$, and we record the waiting times averaged over 100 realisations for different noise amplitude ε. These waiting times have an exponential distribution, correctly predicted by our formula (16), as shown in figure 6(left, red line), while using the original Eyring–Kramers formula, or the mobility correction only leads to mispredictions by a factor approximately 5.

Figure 6(right) shows a single segregation event, in which an initially homogeneous population of agents is driven to segregation by fluctuations that locally deplete the population strong enough for a gap to form, transitioning into the segregated state with a dilute region and an aggregate.

J. Stat. Mech. (2024) 103206

6. Conclusion

We show how recent breakthroughs in the derivation of mean first passage times to leave the basin of attraction of metastable states can be generalised to compute expected waiting times for wide classes of (generalised) gradient flows in the presence of conserved quantities. These generalizations are particularly important when applied to fluctuating hydrodynamics equations, which are limiting equations of interacting particle systems in the limit of many particles.

Such equations are ubiquitous in nature, whenever a large number of interacting agents leads to complex emergent behavior: Apart from molecular dynamics and its applications in chemistry and material design, systems such as traffic flows, pedestrian dynamics, or socioeconomics must follow similar large-scale limits. All these systems usually possess conserved quantities, such as mass or number-of-agents, energy, or momentum, which lead to divergences in the naive application of the limiting equations for mean first passage times due to zero-eigenvectors in the corresponding mobility operator.

Here, we show how we can generalise existing results to incorporate (1) position dependent mobility, (2) degenerate mobility operators including zero-modes, (3) formally the functional setting, where we are applying our results successfully to gradient flows in function spaces. The result is a closed formula for the expected passage times for leaving a locally stable basin of attraction of the stochastic dynamics in the low-noise limit. We demonstrate our results to be applicable in a broad class of settings, including liquid nanofilm rupture times as well as social dynamics with urban segregation. The results are very generally applicable to other systems of the same class, including shallow water flows, Elo dynamics, or traffic flows.

Acknowledgments

TG would like to thank A Donev for interesting discussions. TG acknowledges the support received from the EPSRC Projects EP/T011866/1 and EP/V013319/1. JES acknowledges the support from EPSRC Grants EP/W031426/1, EP/S029966/1 and EP/P031684/1. JBL was supported by a studentship within the EPSRC–supported Centre for Doctoral Training in modeling of Heterogeneous Systems, Grant No. EP/S022848/1. We additionally want to thank the anonymous referee for suggesting the generalization to multiple conserved quantities via restriction to the tangent space. Relevant code used in this paper is openly available at: https://github.com/JingBang-Liu/fluctuating_hydrodynamics_first_passage_time.

Appendix A.

Lemma 1. *Let s be the relevant saddle, and μ_- the unique unstable eigenvector of $M_s H_s$, and $\hat{n}$ the normal vector to ∂B at the saddle. Then*

$$H_s M_s \hat{n} = \mu_- \hat{n}\,, \tag{A.1}$$

J. Stat. Mech. (2024) 103206

i.e. $\hat{n}$ *is an eigenvector of* $H_s M_s$ *with eigenvalue* μ_-.

Proof. Let $V^+ = T_{x_s}\partial B$ be the tangent space to the separatrix at the saddle, which is spanned by the $n-1$ eigenvectors $\{v_i^+\}_{i\in\{1,\dots,n-1\}}$ that correspond to positive eigenvalues μ_i^+ of $M_s H_s$. All these stable eigenvectors are parallel to the separatrix, implying $v_i^+ \cdot \hat{n} = 0$ for all i. Further, denote by v^- the unique unstable eigenvector of $M_s H_s$ with eigenvalue μ_-. Together, the v_i^+ and v^- span all of $\mathbb{R}^n$ and we can write every vector $v \in \mathbb{R}^n$ as

$$v = c^- v^- + \sum_i c_i^+ v_i^+ \quad \text{with} \quad c^-, c_1^+, \dots, c_{n-1}^+ \in \mathbb{R}. \tag{A.2}$$

Then

$$\begin{aligned}
\hat{n} \cdot M_s H_s v &= c^- \hat{n} \cdot M_s H_s v^- + \sum_i c_i^+ \hat{n} \cdot M_s H_s v_i^+ \\
&= \mu_- c^- \hat{n} \cdot v^- + \sum_i c_i^+ \mu_i^+ \underbrace{\hat{n} \cdot v_i^+}_{=0} \\
&= \mu_- \left(c^- v^- \cdot \hat{n} + \sum_i c_i^+ \underbrace{v_i^+ \cdot \hat{n}}_{=0} \right) \qquad = \mu_- v \cdot \hat{n}.
\end{aligned}$$

We conclude

$$v \cdot H_s M_s \hat{n} = \mu_- v \cdot \hat{n}. \tag{A.3}$$

Since (A.3) holds for arbitrary v, we obtain the statement (A.1). □

Lemma 2. *At the saddle,* $x = x_s$,

$$\beta(x_s) = \hat{n} \cdot M_s H_s \hat{n} = \mu_-. \tag{A.4}$$

Proof. Follows immediately from lemma 1. □

Lemma 3. *At the saddle,* $x = x_s$,

$$\mu_- = \frac{\alpha(s)}{\hat{n} \cdot H_s^{-1} \hat{n}}. \tag{A.5}$$

Proof. For $\alpha(s) = \hat{n} \cdot M_s \hat{n}$, we have

$$M_s \hat{n} = \mu_- H_s^{-1} \hat{n} \tag{A.6}$$

from lemma 1. Solving for μ_- yields

$$\mu_- = \frac{\hat{n} \cdot M_s \hat{n}}{\hat{n} \cdot H_s^{-1} \hat{n}} = \frac{\alpha(s)}{\hat{n} \cdot H_s^{-1} \hat{n}}, \tag{A.7}$$

which is the desired result. □

J. Stat. Mech. (2024) 103206

Lemma 4. *Let N be a co-dimension 1 hyperplane in $\mathbb{R}^n$ with normal vector $\hat{n}$, and $H \in \mathbb{R}^{n\times n}$ positive definite. Then, the Gaussian integral, restricted to the hyperplane N, is given by*

$$\int_N e^{-\frac{1}{2}y\cdot Hy}\, d\sigma\,(y) = (2\pi)^{(n-1)/2}\,|\hat{n}\cdot H^{-1}\hat{n}|^{-1/2}|\det H|^{-1/2}. \tag{A.8}$$

Proof. We have

$$\int_{\mathbb{R}^n} \mathrm{e}^{-\frac{1}{2}z\cdot Hz}\,\mathrm{d}z = (2\pi)^{n/2}\,|\det H|^{-1/2}. \tag{A.9}$$

In order to obtain a formula for the restricted Gaussian integral, consider the coordinate change

$$z = y + sH^{-1}\hat{n} \quad \text{with} \quad y\in N, \quad s\in\mathbb{R}. \tag{A.10}$$

Since we can write $H^{-1}\hat{n} = (\hat{n}\cdot H^{-1}\hat{n})\hat{n} + v$, where $v\in N$, we know that the change of variables yields

$$\mathrm{d}z = \mathrm{d}\left(H^{-1}\hat{n}\right)\wedge \mathrm{d}y = |\hat{n}\cdot H^{-1}\hat{n}|\,\mathrm{d}\sigma\,(y)\,\mathrm{d}s. \tag{A.11}$$

Here, $\mathrm{d}\sigma(z)$ is the differential element in the hyperplane N. Thus,

$$\begin{aligned}\int_{\mathbb{R}^n} \mathrm{e}^{-\frac{1}{2}z\cdot Hz}\,\mathrm{d}z &= |\hat{n}\cdot H^{-1}\hat{n}|\int_{\mathbb{R}}\int_N \mathrm{e}^{-\frac{1}{2}\left(y+sH^{-1}\hat{n}\right)\cdot H\left(y+sH^{-1}\hat{n}\right)}\,\mathrm{d}\sigma\,(y)\,\mathrm{d}s\\ &= |\hat{n}\cdot H^{-1}\hat{n}|\left(\int_N \mathrm{e}^{-\frac{1}{2}y\cdot Hy}\,\mathrm{d}\sigma\,(y)\right)\left(\int_{\mathbb{R}} \mathrm{e}^{-\frac{1}{2}s^2\left(\hat{n}\cdot H^{-1}\hat{n}\right)}\,\mathrm{d}s\right)\\ &= (2\pi)^{1/2}\,|\hat{n}\cdot H^{-1}\hat{n}|^{1/2}\int_N \mathrm{e}^{-\frac{1}{2}y\cdot Hy}\,\mathrm{d}\sigma\,(y)\,,\end{aligned}$$

and via equation (A.9) we arrive at the desired result. □

Lemma 5. *Let N and M be two co-dimension 1 hyperplanes in $\mathbb{R}^n$ with normal vectors $\hat{n}$ and $\hat{m}$, respectively, and $H\in\mathbb{R}^{n\times n}$ positive definite. Then, the Gaussian integral, restricted to the intersection of the two hyperplanes $N\cap M$, is given by*

$$\int_{N\cap M} e^{-\frac{1}{2}y\cdot Hy}\,dy = (2\pi)^{(n-2)/2}\,|\hat{n}\cdot H^{-1}\hat{n}|^{1/2}|\hat{m}\cdot H^{-1}\hat{m}|^{1/2}\,(\det H)^{1/2} \tag{A.12}$$

if $\hat{n}$ and $\hat{m}$ are orthogonal in the H^{-1} inner product,

$$\hat{n}\cdot H^{-1}\hat{m} = 0. \tag{A.13}$$

Proof. With a similar argument as before, consider the coordinate change

$$z = y + sH^{-1}\hat{n} + tH^{-1}\hat{m} \quad \text{with} \quad y\in N\cap M, \quad s,t\in\mathbb{R} \tag{A.14}$$

J. Stat. Mech. (2024) 103206

Then, the volume element yields

$$\mathrm{d}z = \mathrm{d}y \wedge \mathrm{d}\left(H^{-1}\hat{n}\right) \wedge \mathrm{d}\left(H^{-1}\hat{m}\right) = \left|\left(\hat{n}\cdot H^{-1}\hat{n}\right)\left(\hat{m}\cdot H^{-1}\hat{m}\right) - \left(\hat{n}\cdot H^{-1}\hat{m}\right)\left(\hat{m}\cdot H^{-1}\hat{n}\right)\right| \mathrm{d}\sigma\left(y\right)\mathrm{d}s\,\mathrm{d}t\,. \tag{A.15}$$

Since by assumption $\hat{n}\cdot H^{-1}\hat{m} = \hat{m}\cdot H^{-1}\hat{n} = 0$, we arrive at the desired result with the same in lemma 4.

□

Lemma 6. *Let $\hat{m}$ be the zero eigenvector of the mobility matrix $M(x_s)$ at the saddle x_s, and $\hat{n}$ the normal vector to the separatrix ∂B at the saddle x_s. Then*

$$\hat{n}\cdot H_s^{-1}\hat{m} = \hat{m}\cdot H_s^{-1}\hat{n} = 0\,. \tag{A.16}$$

Proof. From lemma 1 we know

$$M_s\hat{n} = \mu_- H_s^{-1}\hat{n}\,, \tag{A.17}$$

and thus

$$\hat{m}\cdot H_s^{-1}\hat{n} = \frac{1}{\mu_-}\hat{m}\cdot M\hat{n} = \frac{1}{\mu_-}\hat{n}\cdot M\hat{m} = 0\,. \tag{A.18}$$

□

Lemma 7. *Let N and M_i be co-dimension 1 hyperplanes in $\mathbb{R}^n$ with normal vectors $\hat{n}$ and $\hat{m}_i$, $i = 1,\ldots,k$, respectively, and $H \in \mathbb{R}^{n\times n}$ positive definite. Then, the Gaussian integral, restricted to the intersection of the hyperplanes $N \cap M_1 \ldots \cap M_k$, is given by*

$$\int_{N\cap M_1\ldots\cap M_k} e^{-\frac{1}{2}x\cdot Hx}\,dx = (2\pi)^{(n-k)/2}\left|\hat{n}\cdot H^{-1}\hat{n}\right|^{1/2} \tag{A.19}$$

$$\times \left|\hat{m}_1\cdot H^{-1}\hat{m}_1\right|^{1/2}\ldots\left|\hat{m}_k\cdot H^{-1}\hat{m}_k\right|^{1/2}\left(\det H\right)^{1/2}, \tag{A.20}$$

if $\hat{n}$ and $\hat{m}_i$ are orthogonal in the H^{-1} inner product.

Proof. With a similar argument as before in lemma 5, consider the coordinate change

$$z = y + sH^{-1}\hat{n} + \sum_{i=1}^{k} t_i H^{-1}\hat{m}_i \quad \text{with} \quad y \in N\cap M_1\ldots\cap M_k, \quad s, t_i \in \mathbb{R}.$$

Then, by the assumption that $\hat{n}$ and $\hat{m}_i$ are orthogonal in the H^{-1} inner product, we have the volumen element

$$\begin{aligned}\mathrm{d}z &= \mathrm{d}y \wedge \mathrm{d}\left(H^{-1}\hat{n}\right) \wedge \mathrm{d}\left(H^{-1}\hat{m}_1\right)\ldots\wedge\mathrm{d}\left(H^{-1}\hat{m}_k\right)\\ &= \left|\left(\hat{n}\cdot H^{-1}\hat{n}\right)\left(\hat{m}_1\cdot H^{-1}\hat{m}_1\right)\ldots\left(\hat{m}_k\cdot H^{-1}\hat{m}_k\right)\right|\mathrm{d}\sigma\left(y\right)\mathrm{d}s\,\mathrm{d}t_1\ldots\mathrm{d}t_k,\end{aligned}$$

and we arrive at the desired result with the same in lemma 5. □

J. Stat. Mech. (2024) 103206

Appendix B. Hessian as second variation

In this section we sketch a formal derivation of Hessian of a given energy functional. We first show the derivation of the Hessian of the energy functional of the STF. The functional derivative of the energy functional of STF (21) is given by [47] (here we omit in our notation the t-dependence of h)

$$\frac{\delta E\left[h\left(x\right)\right]}{\delta h\left(x\right)} = \frac{4\pi^2}{3h\left(x\right)^3} - \frac{\partial^2 h\left(x\right)}{\partial x^2}. \tag{B.1}$$

The Hessian we are looking for is formally the functional derivative of the functional derivative. If we rewrite equation (B.1) as an integral,

$$\frac{\delta E\left[h\left(x\right)\right]}{\delta h\left(x\right)} = F\left[h\left(x\right)\right] = \int_0^1 \left(\frac{4\pi^2}{3h\left(x'\right)3} - \frac{\partial^2 h\left(x'\right)}{\partial x'^2}\right)\delta\left(x'-x\right)\mathrm{d}x' \tag{B.2}$$

$$= \int_0^1 f\left(x', h\left(x'\right), \frac{\partial^2 h\left(x'\right)}{\partial x'^2}\right)\mathrm{d}x', \tag{B.3}$$

we can again use the definition of functional derivative [47] to get

$$\int_0^1 \frac{\delta F\left[h\left(x\right)\right]}{\delta h\left(x\right)}\xi\left(x\right)\mathrm{d}x = \left\{\frac{\mathrm{d}}{\mathrm{d}\epsilon}\left(F\left[h\left(x\right)+\epsilon\xi\left(x\right)\right]\right)\right\}_{\epsilon=0} \tag{B.4}$$

$$= \int_0^1 \frac{\partial f}{\partial h}\xi\left(x'\right) + \frac{\partial^2 f}{\partial\left(\partial_{x'}^2 h\left(x'\right)\right)^2}\frac{\partial^2\xi\left(x'\right)}{\partial x'^2}\mathrm{d}x' \tag{B.5}$$

$$= \int_0^1 \xi\left(x'\right)\left(\frac{\partial f}{\partial h} + \frac{\partial^2}{\partial x'^2}\frac{\partial^2 f}{\partial\left(\partial_{x'}^2 h\left(x'\right)\right)^2}\right)\mathrm{d}x' \tag{B.6}$$

$$= \int_0^1 \xi\left(x'\right)\left(-\frac{4\pi^2}{h\left(x'\right)^4}\delta\left(x'-x\right) - \frac{\partial^2}{\partial x'^2}\delta\left(x'-x\right)\right)\mathrm{d}x' \tag{B.7}$$

$$= -\frac{4\pi^2}{h\left(x\right)^4}\xi\left(x\right) - \frac{\partial^2\xi\left(x\right)}{\partial x^2} \tag{B.8}$$

$$= \int_0^1 \frac{\delta^2 E\left[h\left(x\right)\right]}{\delta h\left(x\right)^2}\xi\left(x\right)\mathrm{d}x. \tag{B.9}$$

Here $\xi(x)$ is a periodic test function, the third line used integration by parts, and the fourth line used the properties of Dirac delta functional and its derivatives. The Hessian, $\delta^2 E[h(x)]/\delta h(x)^2$, can be interpreted as an operator on $\xi(x)$, and thus can be discretised and calculated numerically.

Similarly, we can calculate the gradient and the Hessian of the energy functional of the urban segregation model. Equations (24) and (5) give us the following energy functional

$$E\left[\rho\right] = \int_0^1 \left(\rho\log\rho + \left(1-\rho\right)\log\left(1-\rho\right) - \tfrac{1}{2}C\rho^2 - \frac{\kappa^2}{4}C\rho\frac{\partial^2\rho}{\partial x^2}\right)\mathrm{d}x. \tag{B.10}$$

J. Stat. Mech. (2024) 103206

The functional derivative of $E[\rho]$ is

$$\frac{\delta E[\rho]}{\delta \rho} = \log(\rho) - \log(1-\rho) - C\rho - \frac{\kappa^2}{2} C \frac{\partial^2 \rho}{\partial x^2}, \tag{B.11}$$

or in its integral form

$$\frac{\delta E[\rho]}{\delta \rho} = F[\rho] = \int_0^1 f\left(x', \rho(x'), \frac{\partial^2 \rho(x')}{\partial x'^2}\right) \tag{B.12}$$

$$= \int_0^1 \left(\log\left(\frac{\rho(x')}{1-\rho(x')}\right) - C\rho(x') - \frac{\kappa^2}{2} C \frac{\partial^2 \rho(x')}{\partial x'^2}\right) \delta(x'-x)\,\mathrm{d}x'. \tag{B.13}$$

And the Hessian of $E[\rho]$ is given by

$$\int_0^1 \frac{\delta F[\rho(x)]}{\delta \rho(x)} \xi(x)\,\mathrm{d}x$$

$$= \int_0^1 \frac{\partial f}{\partial \rho}\xi(x') + \frac{\partial^2 f}{\partial\left(\partial^2_{x'}\rho(x')\right)^2} \frac{\partial^2 \xi(x')}{\partial x'^2}\mathrm{d}x' \tag{B.14}$$

$$= \int_0^1 \xi(x')\left(\left(\frac{1}{\rho(x')} + \frac{1}{1-\rho(x')} - C\right)\delta(x'-x) - \frac{\kappa^2}{2} C \frac{\partial^2}{\partial x'^2}\delta(x'-x)\right)\mathrm{d}x' \tag{B.15}$$

$$= \left(\frac{1}{\rho(x)} + \frac{1}{1-\rho(x)} - C\right)\xi(x) - \frac{\kappa^2}{2} C \frac{\partial^2 \xi(x)}{\partial x^2} \tag{B.16}$$

$$= \int_0^1 \frac{\delta^2 E[\rho(x)]}{\delta \rho(x)^2}\xi(x)\,\mathrm{d}x. \tag{B.17}$$

Appendix C. Local approximation of convolution

In this section we show the local approximation of convolution with a Gaussian kernel. Given a Gaussian kernel with variance κ^2,

$$K(x) = \frac{1}{\sqrt{2\pi}\kappa}\exp\left(-\frac{x^2}{2\kappa^2}\right), \tag{C.1}$$

we first show that its Fourier transform is also a Gaussian, that is

$$\hat{K}(k) = \int_{-\infty}^{\infty} \exp(-\mathrm{i}kx) K(x)\,\mathrm{d}x = \exp\left(-\frac{\kappa^2 k^2}{2}\right). \tag{C.2}$$

Differentiate the Gaussian kernel gives

$$\frac{\mathrm{d}K}{\mathrm{d}x} = -\frac{x}{\kappa^2}K(x). \tag{C.3}$$

Fourier transform on both side gives

$$\mathrm{i}k\hat{K}(k) = \frac{1}{\mathrm{i}\kappa^2}\frac{\mathrm{d}\hat{K}}{\mathrm{d}k}, \tag{C.4}$$

J. Stat. Mech. (2024) 103206

and so

$$\frac{1}{\hat{K}}\frac{\mathrm{d}\hat{K}}{\mathrm{d}k} = -k\kappa^2. \tag{C.5}$$

Integrating both side from 0 to k gives

$$\ln\left(\hat{K}(k)\right) - \ln\left(\hat{K}(0)\right) = -\frac{k^2\kappa^2}{2}. \tag{C.6}$$

Since the Gaussian kernel is normalised, we know that

$$\hat{K}(0) = \int_{-\infty}^{\infty} K(x)\exp(0)\,\mathrm{d}x = 1, \tag{C.7}$$

and so we have the desired result. Assuming $\kappa^2 \ll 1$, we can then Taylor expand $\hat{K} = 1 - \kappa^2 k^2/2 + \mathcal{O}(\kappa^4)$, and so

$$K(x) = \frac{1}{2\pi}\int_{-\infty}^{\infty}\hat{K}(k)\exp(\mathrm{i}kx)\,\mathrm{d}k = \frac{1}{2\pi}\int_{-\infty}^{\infty}\left(1 - \frac{\kappa^2}{2}k^2 + \mathcal{O}\left(\kappa^4\right)\right)\exp(\mathrm{i}kx)\,\mathrm{d}k. \tag{C.8}$$

Since the Gaussian kernel is symmetric, the convolution is given by

$$K \star \rho = \int_{-\infty}^{\infty}\rho(y)\,K(x-y)\,\mathrm{d}y \tag{C.9}$$

$$= \int_{-\infty}^{\infty}\rho(y)\frac{1}{2\pi}\int_{-\infty}^{\infty}\left(1 - \frac{\kappa^2}{2}k^2 + \mathcal{O}\left(\kappa^4\right)\right)\exp(\mathrm{i}k(x-y))\,\mathrm{d}k\mathrm{d}y \tag{C.10}$$

$$= \int_{-\infty}^{\infty}\frac{1}{2\pi}\hat{\rho}(k)\exp(\mathrm{i}kx)\,\mathrm{d}k - \frac{1}{2\pi}\int_{-\infty}^{\infty}\frac{\kappa^2}{2}k^2\hat{\rho}(k)\exp(\mathrm{i}kx)\,\mathrm{d}k + \mathcal{O}\left(\kappa^4\right) \tag{C.11}$$

$$= \rho(x) + \frac{\kappa^2}{2}\partial_x^2\rho(x) + \mathcal{O}\left(\kappa^4\right). \tag{C.12}$$

References

[1] Brinkman B A W, Yan H, Maffei A, Park I M, Fontanini A, Wang J and La Camera G 2022 *Appl. Phys. Rev.* **9** 011313
[2] Garcia E R and Hofmann J 2024 *Phys. Rev.* E **109** L032103
[3] Ashwin P and von der Heydt A S 2020 *J. Stat. Phys.* **179** 1531–52
[4] Lohmann J, Dijkstra H A, Jochum M, Lucarini V and Ditlevsen P D 2024 *Sci. Adv.* **10** eadi4253
[5] Bashkirtseva I and Ryashko L 2011 *Chaos* **21** 047514
[6] Bovier A, Eckhoff M, Gayrard V and Klein M 2004 *J. Eur. Math. Soc.* **6** 399–424
[7] Arrhenius S 1889 *Z. Fuer Phys. Chem.* **4** 226–48
[8] Freidlin M I and Wentzell A D 2012 *Random Perturbations of Dynamical Systems* vol 260 (Springer)
[9] Eyring H 1935 *J. Chem. Phys.* **3** 107–15
[10] Kramers H A 1940 *Physica* **7** 284–304
[11] Berglund N 2013 *Markov Process. Relat. Fields* **19** 459–90
[12] Bouchet F and Reygner J 2016 *Ann. Henri Poincare* **17** 3499–532
[13] Landim C and Seo I 2018 *Commun. Pure Appl. Math.* **71** 203–66
[14] Landim C, Mariani M and Seo I 2019 *Arch. Ration. Mech. Anal.* **231** 887–938

J. Stat. Mech. (2024) 103206

[15] Jordan R, Kinderlehrer D and Otto F 2006 *SIAM J. Math. Anal.* **29** 1–17
[16] Berglund N and Gentz B 2010 *Markov Process. Relat. Fields* **16** 549–98
[17] Gardiner C 2009 *Stochastic Methods: a Handbook for the Natural and Social Sciences* (Springer)
[18] Bedeaux D and Mazur P 1974 *Physica* **76** 247–58
[19] Dean D S 1996 *J. Phys. A: Math. Gen.* **29** L613
[20] Landau L D and Lifshitz E M 2007 *Lehrbuch der Theoretischen Physik VI - Hydrodynamik* 5th edn (Verlag Harri Deutsch)
[21] Fehrman B and Gess B 2023 *Invent. Math.* **234** 573–636
[22] Djurdjevac A, Kremp H and Perkowski N 2024 *Stoch. PDE: Anal. Comput.* **12** 2330–55
[23] Weinan W and Zhou X 2011 *Nonlinearity* **24** 1831
[24] Kasdin N J 1995 *J. Guid. Control Dyn.* **18** 114–20
[25] Weinstein S J 2004 *Annu. Rev. Fluid Mech.* **36** 29–53
[26] Karnik R, Fan R, Yue M, Li D, Yang P and Majumdar A 2005 *Nano Lett.* **5** 943–8
[27] Makarov S V, Milichko V A, Mukhin I S, Shishkin I I, Zuev D A, Mozharov A M, Krasnok A E and Belov P A 2016 *Laser Photonics Rev.* **10** 91–99
[28] Herminghaus S, Jacobs K, Mecke K, Bischof J, Fery A, Ibn-Elhaj M and Schlagowski S 1998 *Science* **282** 916–9
[29] Xie R, Karim A, Douglas J F, Han C C and Weiss R A 1998 *Phys. Rev. Lett.* **81** 1251–4
[30] Seemann R, Herminghaus S and Jacobs K 2001 *Phys. Rev. Lett.* **86** 5534–7
[31] Nguyen T D, Fuentes-Cabrera M, Fowlkes J D and Rack P D 2014 *Phys. Rev.* E **89** 032403
[32] Zhang Y, Sprittles J E and Lockerby D A 2019 *Phys. Rev.* E **100** 023108
[33] Sprittles J E, Liu J, Lockerby D A and Grafke T 2023 *Phys. Rev. Fluids* **8** L092001
[34] Ruckenstein E and Jain R K 1974 *J. Chem. Soc. Faraday Trans.* 2 **70** 132
[35] Grün G, Mecke K and Rauscher M 2006 *J. Stat. Phys.* **122** 1261–91
[36] Durán-Olivencia M A, Gvalani R S, Kalliadasis S and Pavliotis G A 2019 *J. Stat. Phys.* **174** 579–604
[37] Cox S and Matthews P 2002 *J. Comput. Phys.* **176** 430–55
[38] Manacorda A and Puglisi A 2017 *Phys. Rev. Lett.* **119** 208003
[39] Chu K C, Yang L, Saigal R and Saitou K 2011 Validation of stochastic traffic flow model with microscopic traffic simulation *2011 IEEE Int. Conf. Automation Science and Engineering* pp 672–7
[40] Carrillo J A, Martin S and Wolfram M T 2016 *Math. Models Methods Appl. Sci.* **26** 671–97
[41] Aurell A and Djehiche B 2019 *Transp. Res.* B **121** 168–83
[42] Zakine R, Garnier-Brun J, Becharat A C and Benzaquen M 2024 *Phys. Rev.* E **109** 044310
[43] Schelling T C 1971 *J. Math. Sociol.* **1** 143–86
[44] Sakoda J M 1971 *J. Math. Sociol.* **1** 119–32
[45] Grauwin S, Bertin E, Lemoy R and Jensen P 2009 *Proc. Natl Acad. Sci.* **106** 20622–6
[46] Burger M, Pietschmann J F, Ranetbauer H, Schmeiser C and Wolfram M T 2022 *Eur. J. Appl. Math.* **33** 111–32
[47] Parr R G and Weitao Y 1995 *Density-Functional Theory of Atoms and Molecules* (Oxford University Press)

J. Stat. Mech. (2024) 103206